Mechanically Stimulated Cytoskeleton Rearrangement and Cortical Contraction in Human Neutrophils

Doncho V. Zhelev and Robert M. Hochmuth
Department of Mechanical Engineering and Materials Science, Duke University, Durham, North Carolina 27708–0300 USA

ABSTRACT A mechanical test with micropipets is used to characterize cytoskeleton rearrangement and contraction induced by mechanical stresses in human neutrophils. The yield shear resultant of the cell cortex is on the order of 0.06 to 0.09 $mN \cdot m^{-1}$. The measured yield shear resultant suggests that the neutrophil cortex is a weakly cross-linked structure. When a tether is pulled out from the cell surface, a polymer structure starts to fill it and spreads out from the cell body. The rate of advancement of the polymerization front is almost constant and, therefore, is not diffusion limited. The measured rate is much smaller than the one of spontaneous actin polymerization, suggesting that the limiting process is either the dissociation of actin monomers from their dimers with the capping proteins or the rate of formation of new nucleation sites or both. Polymerization is also observed after applying sufficient mechanical stresses on a small portion of the cell surface. The polymerization is followed by mass transfer from the cell into the prestressed region and later on by contraction of the main cell body. The pressure generating the flow is located in the prestressed region and most probably is a result of its "swelling" and contraction. The contraction of the main cell body is very similar (in its time dependence and magnitude) to the contraction during phagocytosis. The measured maximum cortical tension is on the order of 0.5 $mN \cdot m^{-1}$, which for a 3.5-μm diameter pipet corresponds to a maximum contraction force of 11 nN.

INTRODUCTION

The neutrophil, as a part of the body's defense system, is found in two major states: resting and activated. The characterization of the mechanical properties of the resting state has been a focus of a number of studies in the past decade. They have shown that the cell resembles a fluid body with a persistent tension in its surface (Evans and Kukan, 1984; Evans and Yeung, 1989; Needham and Hochmuth, 1990; Tran-Son-Tay et al., 1991). The tension originates from the cortical meshwork (Stossel et al., 1980), which has been revealed by characterizing the neutrophil's resistance to deformation at high curvatures (Zhelev et al., 1994). The mechanical properties of the cell during activation, however, are still not well characterized. Recently, two methods have emerged, one for studying leukocyte phagocytosis (Evans et al., 1993) and another for characterizing its locomotion (Usami et al., 1992). In comparison with the other methods for studying active leukocyte behavior, these two methods allow one to perform force measurements. The measured forces for contraction during phagocytosis and the "thrust" force in locomotion are on the same order of magnitude as the ones exerted by other nonmuscle cells during their active motions (Oliver et al., 1994; Evans, 1993).

Phagocytosis experiments show that there are at least three distinguishable stages of this process (Evans et al., 1993): 1) adhesion, 2) polymerization and lamellipodia advancement, and 3) contraction of the cell body. The two latter stages, polymerization and contraction, are closely related to changes in the cortical network (Stossel et al., 1980). It is thought that the polymerization is regulated both by factors providing the available free monomers in the vicinity of the nucleation sites and by factors affecting the affinity of the monomers to bind to these nucleation sites. There are a number of studies that have identified and characterized the molecules involved in this process (Stossel, 1982; Geiger, 1983; Hartwig et al., 1985; Pollard and Cooper, 1986; Hartwig and Kwiatkowski, 1991). The current view is that successful polymerization requires also the existence of nucleation sites. Inside the cell they may be generated by spontaneous formation of new nucleation sites or by creating barbed ends by severing the existing F-actin filaments (Luna, 1991). The contraction stage is poorly studied, probably because of the lack of a quantitative method for its characterization. The presence of myosin suggests that both the persistent cortical tension in the resting neutrophil as well as its contraction in the active state involves the actin-myosin motor (Stossel et al., 1980; Southwick and Stossel, 1983). In vitro studies (Janson et al., 1991) in the presence of myosin show that a minimum structure is necessary to transmit the generated contraction force. The importance of cortical cross-linking for cell locomotion is demonstrated in vivo by using cells deficient in actin-binding protein, which is the major cross-linking molecule of the leukocyte (Cunningham et al., 1992).

The common way of producing barbed ends, as nucleation sites, is by using chemotactic factors. Recently, it has been shown that cell polarization and actin polymerization may also be induced during cell adhesion (Southwick et al., 1989; Andre et al., 1990). Mechanical deformation, which has been shown to be coupled with an increase in the level of the

Received for publication 25 July 1994 and in final form 30 January 1995.
Address reprint requests to Dr. Doncho V. Zhelev, Department of Mechanical Engineering and Materials Science, Duke University, Durham, NC 27708–0300. Tel.: 919-660-5372; Fax: 919-660-8963; E-mail: dvzh@acpub.duke.edu.

Permanent address of D. V. Z. is Central Laboratory of Biophysics, Bulgarian Academy of Sciences, 1113 Sofia, Bulgaria.

0006-3495/95/05/2004/11 $2.00

intracellular calcium (Horoyan et al., 1990; Zafran et al., 1993), also leads to polymerization and shape changes (Horoyan et al., 1990; Zhelev and Hochmuth, 1994).

The focus of this study is the mechanical behavior of the human neutrophil after application of extreme stresses in a local region of its surface. Since the area of the membrane is about 2–2.5 times the surface area of the cell (Evans and Yeung, 1989; Ting-Beall et al., 1993), the strains related to the applied stresses probably are larger than the maximum possible adjustment of the cortical filaments. Therefore, some of the bonds in the network break and serve as nucleation sites for polymerization. The cascade of events, triggered by the applied stresses, is characterized by measuring the velocities and magnitudes of the observed shape and volume changes as well as the generated forces.

MATERIALS AND METHODS

Cell preparation

The preparation of neutrophils has been described elsewhere (Zhelev et al., 1994). Briefly, venous blood was drawn from healthy adult donors into vacutainers containing EDTA or lithium heparin as an anticoagulant. When the anticoagulant was EDTA, the neutrophils were separated on a Ficoll-Histopaque gradient (Sigma Histopaque-1077 and 1119, Sigma Chemical Co., St. Louis, MO) at 800 *g* for 20 min. The cells were collected at the 1077/1119 interface and washed once with Ca^{2+} and Mg^{2+} free modified Hanks' balanced salt solution (HBSS), (Sigma Chemical Co.). Finally, the cells were resuspended in a 50% autologous plasma/HBSS solution. When the anticoagulant was heparin, the cells were separated using mono-poly resolving medium (ICN Biomedicals Inc., Aurora, OH) and Sigma Histopaque-1119 (Sigma Chemical Co.). After separation, the cells were resuspended in a solution containing 50% autologous plasma and 50% RPMI 1640 (Sigma Chemical Co.). All the procedures and the experiment were done at 23°C.

Micromanipulation

The experimental chamber was 2 mm thick and open from both sides to allow micromanipulation. The bottom of the chamber was covered with a coverslip, and the top was covered with two parallel glass strips with a 1 mm thick gap. Thermostated water was allowed to flow in the gap for temperature control. The cells were observed with an inverted Leitz microscope with a 100× oil immersion objective. Micropipets were made from 0.75-mm capillary glass tubing pulled to a fine point with a vertical pipet puller and were cut to the desired diameter with a microforge. The radii for small pipets were measured from their outside pipet diameters as described elsewhere (Zhelev et al., 1994). The pipets were filled with the solution used in the experiments and were kept in the chamber for 15 min before starting the experiments to minimize cell adhesion to the glass surface (Evans and Kukan, 1984). They were connected to a manometer system, with which the pipet-chamber pressure difference could be controlled between 0.5 and 100 Pa using the micrometer-driven displacement of a water-filled reservoir, or up to 40 kPa using a syringe. The pressures were measured with a differential pressure transducer (Validyne DP15–24, Northridge, CA). The pressure transducer readings together with a time counter (Vista Electronics, Model 401, La Mesa, CA) were multiplexed on the recorded images. Distances were measured with video calipers (Vista Electronics Model 305). For intensity measurements the images were digitized with an image grabber (Neotech Ltd., Hampshire, UK) in a Macintosh II computer and analyzed with National Institutes of Health Image 1.43 (NIH, Bethesda, MD). Transmission light experiments were recorded using a Hamamatsu CCD camera (Hamamatsu Photonics, Japan). Fluorescence images were observed with a Hamamatsu SIT camera.

In the experiments a single "resting" cell, showing an optically smooth surface and uniform diffraction pattern, was chosen and manipulated. The first sign of polymerization, in a good-quality optical image, was the change of the refractive index in the membrane domain where a pseudopod eventually forms.

Cell fixation and staining of F-actin with phallacidin

Single cells were fixed and stained in the experimental chamber. Initially each cell was manipulated using two pipets. At the desired time, the cell was fixed by flowing over it a solution containing 10% formalin from a third pipet. The cell was left in the fixing solution for ½ h. Then it was transferred for 1 h into another chamber containing HBSS, 10 U/ml BODIPY phallacidin (Molecular Probes, Inc., Eugene, OR) and 100 mg/ml monooleoylphosphatidylcholine (Sigma Chemical Co.). Finally the cell was transferred back to the first chamber, which had been washed and filled with PBS, and its fluorescence was observed.

RESULTS

Polymerization and contraction related to tether formation

When a neutrophil is sucked into a pipet it shows an elastic resistance until its surface forms a hemisphere inside the pipet. Then it flows into the pipet as a liquid body (Evans and Kukan, 1984). The simplest model of a neutrophil in a resting state is a sphere filled with a highly viscous liquid and having a uniform cortical tension at its surface. The pressure for formation of a hemispherical projection inside the pipet is called the critical pressure. For pressures above the critical pressure, the cell retains its liquid nature even for pipets having radii on the order of a fraction of a micrometer (Zhelev et al., 1994; Zhelev and Hochmuth, 1994). When the suction pressure is much larger than the critical pressure, there is an additional tension along the cylindrical portion of the membrane inside the pipet (Zhelev and Hochmuth, 1994) due to friction between the membrane and the pipet surface and friction at the mouth of the pipet. This tension is a function of the applied suction pressure and the pipet diameter and is larger for smaller pipets. The minimum size of the pipets used in this study, with radii on the order of 0.4 μm, was chosen to be large enough to allow some of the granules to flow into the pipet. The ability of the granules to flow into the pipet indicates that the thickness of the cortex is smaller than the pipet radius. With increasing suction pressure the maximum induced tension in the cell cortex becomes sufficient to induce a "necking" instability and the formation of a tether (Fig. 1). It is seen from Table 1 that the suction pressure for tether formation is on the order of 600–900 Pa. This pressure gives a maximum pulling force on the order of 0.3–0.45 nN, which for the 0.4 μm pipet used in the experiments corresponds to maximum applied tension in the cortex on the order of 0.12–0.18 $mN \cdot m^{-1}$.

When the tether is formed, its length increases. The increase of the tether length can be stopped by decreasing the suction pressure. The suction pressure required to keep the length of the tether constant in a 0.4-μm radius pipet is on the order of 20 Pa. The total pulling force found from this

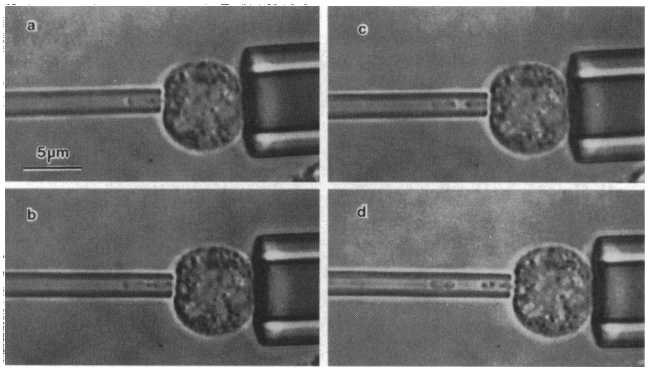

FIGURE 1 Suction of a portion of a neutrophil into a 0.4-μm radius pipet. Initially the cell starts to flow into the pipet (*a*). For high suction pressures the cortical-membrane complex, supporting the cell surface in the pipet, fails (*b*), and a tether is formed (*c*). (Note: the tether cannot be seen.) There is a "plug" at the leading edge of the tether (*c* and *d*) with a length on the order of 2 μm (see Table 1).

TABLE 1 Percent of neutrophils that have a cylindrical shape, or form a neck or tether, when sucked into a 0.4-μm radius pipet using different suction pressures

ΔP (Pa)	Cylinders (%)	Necks (%)	Tethers (%)	Total number of cells	"Plug" length (μm)
600	73	16	11	37	1.60 ± 0.24
900	30	13	57	23	1.86 ± 0.37
1200	19	20	69	74	1.98 ± 0.33
1500	8	23	79	13	2.23 ± 0.40
1800	9	15	76	34	2.17 ± 0.40
2000	6	12	82	16	2.07 ± 0.13

The "plug" length is the total length of the sausage-like portion of the cell at the leading edge of the tether (see Fig. 1).

pressure is an upper estimate of the true force, because the portion of the cell at the leading edge of the tether does not seal the pipet completely. The corresponding tension in the tether membrane may be estimated if its radius is known. However, the radius of the tether is not directly measurable. It may be assumed that it is on the order of 0.02 μm, which is the measured radius of a tether pulled from red blood cells in similar conditions (Waugh and Hochmuth, 1987). Then, the applied membrane tension in the tether region is on the order of 0.08 $mN \cdot m^{-1}$ or less.

Pulling tethers from a neutrophil causes spontaneous polymerization in a local region around the perturbed cell surface. When the tether is released, immediately after its formation, its membrane is pulled back into the neutrophil surface (probably by forces produced by the cortical tension). When the tether is kept stretched for 15–20 s or more, its length remains almost constant after the suction pressure is set equal to zero, or even when the tether is released from the pipet. The tethered region is stiff when it is probed by the pipet. The stiffening of the tether suggests that its shape is supported by a polymer (possibly F-actin) structure. In this case, the tether is "pulled" back to the cell surface in a much slower process, which usually takes minutes, depending on its initial length. At the place of attachment to the cell body, the tether is thicker and the refractive index of the cell surface around this region has changed. The thicker region usually extends 3–4 μm from the cell surface and is stiff, suggesting that its shape is also supported by a highly cross-linked underlying structure.

In a different experiment, the tether and cell are held with two pipets, and a constant pulling force is applied, preventing in this way the "contraction" of the tether into the cell surface. In this case, the thickening of the tether increases along its length (Fig. 2). There is a distinguishable front or leading edge of the polymerized region moving along the tether. The rate of advance of the front is almost constant (Fig. 3) and is independent of the tether length. The average rate of spreading of the polymerization front, found from five cells, is 0.070 ± 0.011 $\mu m \cdot s^{-1}$. The same effect is observed when the tether is formed by allowing the cell to adhere to a surface of zymosan yeast. The tether is formed by separating the cell and the yeast (not shown). In both cases, the polymerization front spreads from the cell surface to a distance up to 10–20 μm or until it reaches the small pipet or yeast particle. When the polymerization front cannot reach the yeast surface or the small pipet, it advances until reaching its maximum distance from the cell and then starts to depolymerize. The polymer structure in the tether region apparently retracts to the cell body and almost all material from the tether region is transported back to the cell. The initiation of both the front advancement and its retraction is an abrupt process, whereas the front movement occurs at a constant rate.

The case in which the polymerization front reaches the small pipet is illustrated in Fig. 2. During the advancement of the polymerization front the cell body is kept at low pressure outside the holding pipet (Fig. 2, *a* and *b*). This is done to provide the necessary support for the cell, because the contraction of the tether region (if there is any) is negligible. After the polymerization front reaches the small pipet and the thickness of the tether region starts to increase, the cell is deformed into the holding pipet (Fig. 2 *c*). A few hundred

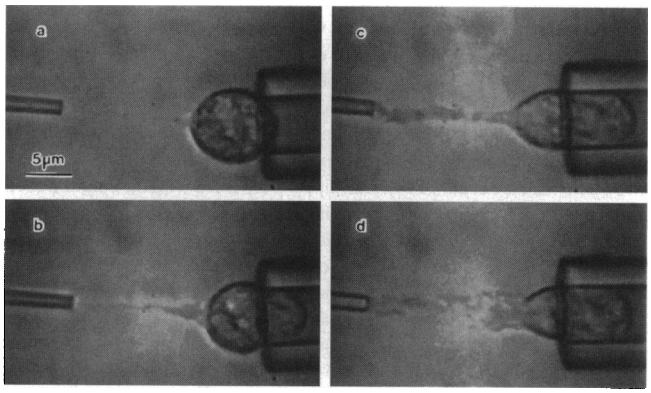

FIGURE 2 Polymerization inside a tether. The tether is formed and its length is kept constant with the help of the small pipet (*a*). Seconds later, a polymer structure starts to "fill" the tether from the cell body (*b*). The rate of spreading of the polymerization front is almost constant (Fig. 3). After the polymerized region reaches the small pipet its thickness starts to increase (*c*). While the thickness of the polymerized region increases the cell starts to contract (*d*) with almost a constant rate of increase of the contraction force (Fig. 3).

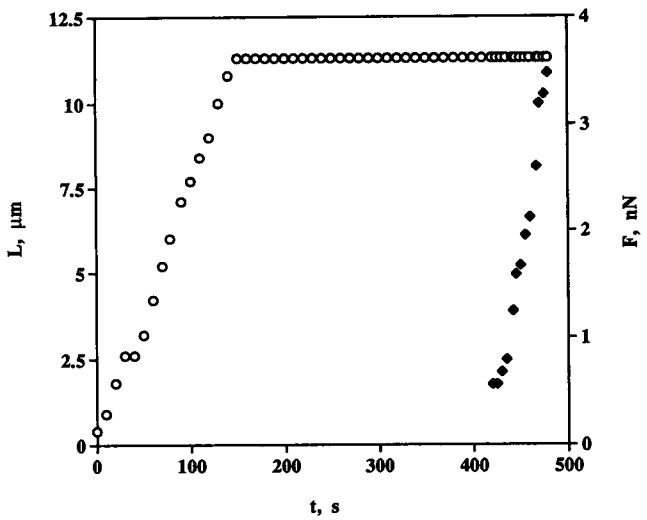

FIGURE 3 Spreading of a polymerization front along a tether (○) and the cell contraction force (♦), versus time. The rate of spreading and the rate of increase of the contraction force are almost constant. The maximum contraction force when the cell is manipulated with two pipets cannot be measured, because the suction pressure in the small pipet becomes sufficient to form a new tether.

seconds later, the cell starts to contract (Fig. 2 *d*). (The delay of the contraction phase depends on the tether length and is smaller for shorter tethers. This dependence was not studied systematically.) After the contraction has started the suction pressure in the two pipets is changed to keep the overall length of the cell and tether constant. During the contraction measurements the cell body has the geometry shown in Fig. 2 *d*. The contraction force increases almost linearly with time (Fig. 3). The rate of increase is on the order of 60 $pN \cdot s^{-1}$, which is close to the rate of increase, 150 $pN \cdot s^{-1}$, of neutrophil contraction in phagocytosis (Evans et al., 1993). When the cell is released from the pipets, it returns to its initial spherical shape in minutes. Polymerization inside tethers may be induced many times in the same neutrophil, and the cell always returns to its initial spherical shape.

Polymerization and contraction related to stretched cylinders

There is evidence that mechanical stresses much smaller than the ones sufficient to pull tethers may alter the mechanical properties of the neutrophil. Experiments with 1–1.25-μm radii pipets show that when the suction pressure exceeds 60 Pa the portion of the cell inside the pipet starts to stiffen and behaves as an elastic body (Zhelev and Hochmuth, 1994). The elastic resistance induced in this experiment is either a function of the applied stress or of the resulting strain. The stresses and the related strains are maximum for pipets having radii on the order of 0.35–0.6 μm (pipets of this size are large enough not to "filter" the granules from the cell cytoplasm). Initially the cell flows into the pipet as a liquid until its flow eventually ceases. The cell is kept under a maximum stress, on the order of 0.2 $mN \cdot m^{-1}$, for 10–30 s. (A possible dependence of the neutrophil response on the time of application of mechanical stress was not studied.) The cytoplasm of the portion of the cell sucked into the pipet is probably a liquid, because the Brownian motion of the trapped granules is observed. The shape of the prestressed region is cylindrical immediately (<2–3 s) after being released from the small pipet. It is stiff, which is shown by the deformation of the cell body when the prestressed region is pressed against it. It starts to thicken in seconds (Fig. 4), and its refractive index becomes similar to the one for pseudopods. While increasing the thickness of the prestressed region, the shape starts to change and form a "pocket" in its middle. A mass flow is observed from the main cell body into the pocket. The main cell body and the pocket are connected with a neck having the shape of a nozzle. The radius of the nozzle increases as the volume of the prestressed region increases. Finally the nozzle disappears and the cell forms a single body, which eventually returns to its initial spherical shape.

The difference of the refractive index in the prestressed region and the nozzle from that of the main cell body suggests that in the former regions there is a cross-linked, dense structure that excludes the plasma granules. Staining of different cells with fluorescent phallacidin at the different stages of the polymerization process (Fig. 5) reveals that the prestressed region and the nozzle are rich in F-actin. The prestressed region shows maximum fluorescence just before the flow starts. When the flow is at the middle of its time course, the maximum fluorescence is observed in the nozzle region, while the fluorescence of the prestressed region decreases. This suggests that the density of the F-actin in the nozzle region remains relatively high even as it decreases in the prestressed region.

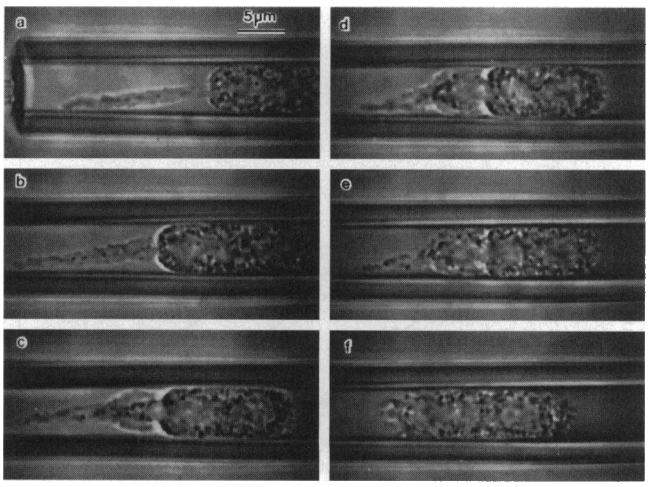

FIGURE 4 Polymerization in a prestressed region. A small portion of a neutrophil is subjected to high tension for 15 s (*a*). After its release, the refractive index of the prestressed region changes and becomes similar to that of a pseudopod (*a* and *b*). The prestressed region swells (*b*) and a "pocket" is formed in its middle, which is connected to the main cell body by a nozzle (*c*). Mass flows from the cell body into the "pocket", which is coupled to an increase in the nozzle diameter (*c–e*). The nozzle disappears, and the cell forms a single body (*f*) and eventually returns to its initial shape. During the mass flow there is a thick "shell" of polymer close to the membrane in the prestressed region, which excludes granular structures (*c–e*).

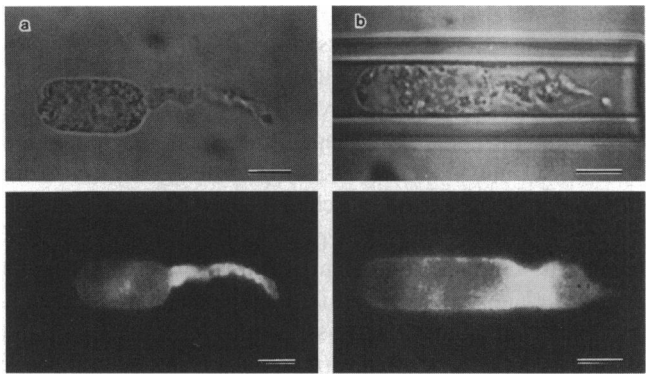

FIGURE 5 Phallacidin-stained leukocytes. (*a*) Prestressed cell, fixed just before the initiation of mass flow. (*b*) Prestressed cell, fixed at the middle of the time course of the mass flow (bars are 5 μm).

The amount of mass transferred from the main cell body into the prestressed region is measured when the cell body is completely sucked into a large reference pipet (Fig. 4). The body of the cell in this case has a "sausage" shape with the cross-sectional diameter determined by the pipet. This configuration allows a precise measurement of the volume changes of the main cell body by measuring its length inside the pipet (Fig. 6). The increase of the thickness of the stressed region starts some seconds after its release from the small pipet. The initial increase of its diameter and the related decrease of the volume of the main body is not coupled with granular transport across the nozzle, probably because the polymer structure in this region is filtering the cytoplasm. The first measurable volume changes are observed 30–40 s after the cell is released from the small pipet. The nozzle is formed 10–20 s later, and the granules start to flow into the prestressed region. Using the granules as markers, it is possible to determine the inside diameter of the nozzle (Fig. 7). The measured volume changes (or the rate of volumetric flow) and the radius of the nozzle can be related to determine the apparent pressure difference causing the flow of the cytoplasm.

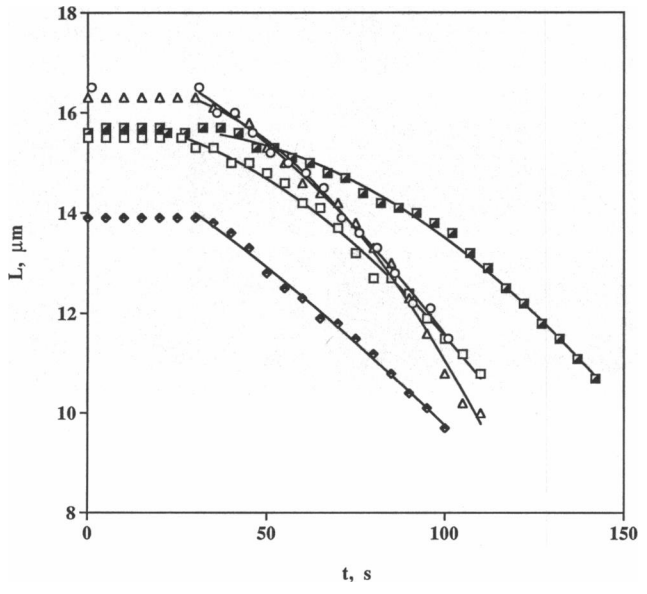

FIGURE 6 Length of the main cell body inside the holding pipet versus time, which measures the volume changes of the cell body during mass flow. Different symbols stand for different cells.

For flow through a nozzle at low Reynolds numbers (Happel and Brenner, 1986), the rate of volumetric flow Q and the nozzle diameter d determine the pressure drop across the nozzle ΔP relative to the fluid viscosity μ and vice versa:

$$\frac{\Delta P}{\mu} = \frac{24Q}{d^3(1 + 2\cos\eta)(1 - \cos\eta)^2} \tag{1}$$

where $\eta = \pi/3$ is the angle defining the hyperboloid that approximates the nozzle (Fig. 8). Fig. 9 shows the predicted values of the ratio of the pressure difference to the cytoplasm viscosity versus time for different cells.

The above ratio may be found independently from velocity measurements using granules as markers. The divergent part of the nozzle can be approximated with a truncated cone characterized by an angle θ that corresponds to η. In this case the velocity of the cytoplasm at a given point is found from the measured velocity of single granules. The velocity of the flow along the axis of symmetry at a distance r from the origin, $v(r)$ (see Fig. 8) is related to the difference in the static pressure at r and at infinity $(\Delta P)_r$, and to the cytosol viscosity μ (Happel and Brenner, 1986)

$$\frac{(\Delta P)_r}{\mu} = \frac{4v(r)}{3r(1 - \cos^2\theta)}. \tag{2}$$

The velocity of the flow at the axis of symmetry $v(r)$ and the rate of volumetric flow Q are given also by Happel and Brenner (1986):

$$v(r) = \frac{3Q(1 + \cos\theta)}{2\pi r^2(1 + 2\cos\theta)(1 - \cos\theta)}. \tag{3}$$

Substituting Eq. 3 into Eq. 2 and dividing Eq. 2 into Eq. 1

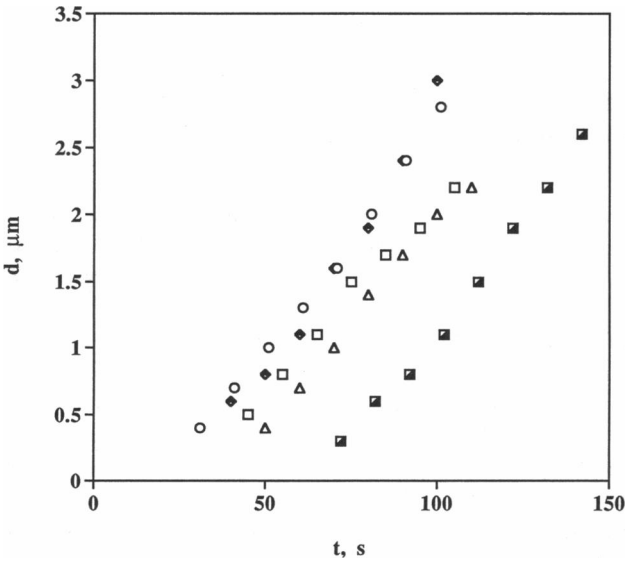

FIGURE 7 Nozzle diameter versus time for the same cells as in Fig. 6.

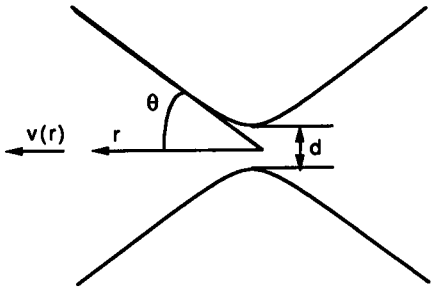

FIGURE 8 Nozzle geometry. The angle η, characterizing the hyperboloid, is equal to $\pi/3$ and its diameter is d. The divergent part of the nozzle is approximated with a cone with angle $\theta = \eta$.

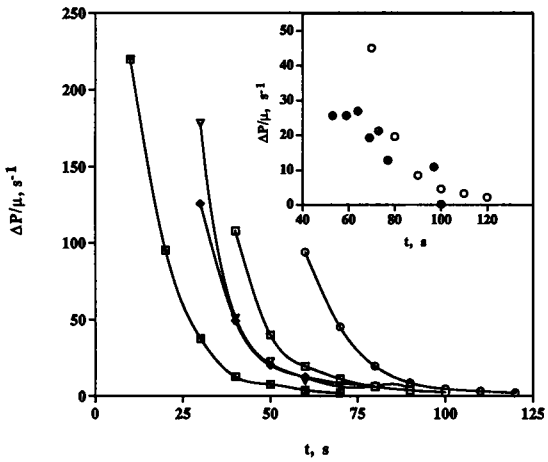

FIGURE 9 The ratio of the pressure difference across the nozzle to the cytosol viscosity versus time (different symbols stand for different cells). The ratio is found from Eq. 1 and experimental measurements of Q and d. In the insert is shown the same ratio for one of the cells determined from the velocity measurements at a given r by using Eqs. 2 and 4. The total nonperturbed movement of the granules during their flow through the nozzle is over a distance of 5–7 μm. The velocities are determined from measurements over a distance ≤ 1 μm at the middle of the above interval. (It was calculated that the relaxation distance for a granule to approach the free stream velocity was only 1 Å.)

gives (because Q is the same in either case):

$$\frac{\Delta P}{\mu} = \frac{12\pi r^3}{d^3}\frac{(\Delta P)_r}{\mu}. \tag{4}$$

Thus, measuring the velocity of granular movement at a given r gives a value for $[(\Delta P)_r/\mu]$ from Eq. 2 and an independent calculation for the ratio $(\Delta P/\mu)$ from Eq. 4. This independent calculation is plotted on an insert in Fig. 9. It is seen that the two independent estimates of the ratio are in good agreement. The ratio $(\Delta P/\mu)$ decreases with time, and its final values are two orders of magnitude smaller than the initial ones.

The flow measurements are consistent with the static pressure in the prestressed region being lower than that in the main cell body. However, they do not provide information about the actual values of the pressures in the two regions. The surface of the main cell body, the unstressed portion of the cell, remains smooth, suggesting that it is under isotropic contraction just as is the surface of the resting neutrophil. Therefore, the changes of the static pressure inside the main cell body may be characterized by measuring the apparent cortical tension. The apparent cortical tension, during mechanically stimulated polymerization and mass flow, is measured in an experiment with the following design: 1) the body of the neutrophil is partially sucked into a 2-μm radius pipet (Fig. 10); 2) the opposite side of the cell is sucked into a small pipet and subjected to a high stress for 15 s; 3) the cell is released from the small pipet, and the pressure in the holding pipet is changed to keep the projection length of the neutrophil inside the pipet constant. The apparent cortical tension T is calculated from the law of Laplace (Evans and Skalak, 1980) using the measured suction pressure and the radius of curvature of the cell body outside the pipet:

$$T = \frac{\Delta P}{2\left(\frac{1}{R_p} - \frac{1}{R_{out}}\right)} \tag{5}$$

where ΔP is the pressure difference between the pipet and the chamber, and R_p and R_{out} are the pipet radius and the outside

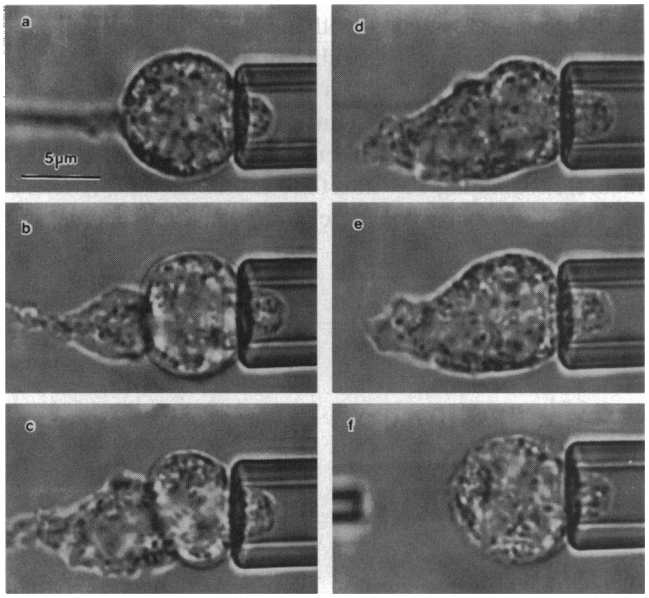

FIGURE 10 Measuring the cortical tension of the main cell body after applying a large mechanical stress to a small portion of the cell. Initially the cell is aspirated into the measuring pipet by applying a suction pressure that is larger than the critical pressure. When the desired projection length is reached the suction pressure is lowered and the projection length is kept stationary. (For projection lengths larger than the pipet radius the "stationary" pressure is smaller than the critical pressure.) Then a high stress is applied to a small portion of the cell by using a small pipet. The cell is released from the small pipet, and the suction pressure in the measuring pipet is changed to keep the projection length constant. The apparent tension is calculated by using Eq. 5 as described in the Results section. The apparent tension immediately after releasing the cell from the small pipet is close to that of the resting neutrophil (a). When mass flow starts, the apparent cortical tension starts to increase (b). It increases and reaches its maximum when the nozzle disappears (c). The cortical tension decreases (d) and the cell eventually returns to its initial spherical shape (e and f).

cell radius, respectively. The pressure difference, the radius of the pipet, and the outside cell radius are measured independently.

The law of Laplace, as expressed in the form given by Eq. 5, has several assumptions including that the interior is liquid and the surface (or the cell membrane) bounding this liquid has equal and constant principal curvatures. Clearly, the hemispherical portion of the cell inside the pipet is the dominant term in Eq. 5. This internal curvature, $1/R_p$, is typically about twice that of the external curvature, $1/R_{out}$. However, the curvatures of the membrane external to the pipet are not equal in Fig. 10 *d*, *e*, and possibly *c*. These curvatures are altered because of the changing boundary conditions in a solid-like domain where the "pseudopod" is being formed and dissolved. It would be possible to derive a law of Laplace that would account for these different curvatures. However, because the external curvatures play a less significant role in Eq. 5 than the internal curvature, the external curvature is approximated by measuring the average value for the radius of curvature of the membrane that bounds the outside liquid portion of the cell shown in Fig. 10, *c–e*.

Fig. 11 shows the measured cortical tension for different cells. The initial cortical tension is on the order of 0.03 $mN \cdot m^{-1}$. The cortical tension starts to increase 40–100 s after releasing the cell from the small pipet, which corresponds to a 20–40-s delay compared with the initiation of cytoplasmic flow. The rate of increase of the cortical tension is from 4×10^{-3} to 1.5×10^{-2} $mN \cdot m^{-1} \cdot s^{-1}$. It reaches its maximum in another 50–70 s. The maximum cortical tension for Ca^{2+} free media is 0.495 ± 0.306 $mN \cdot m^{-1}$ (from 24 cells), and for a medium containing Ca^{2+} it is 0.27 ± 0.22 $mN \cdot m^{-1}$ (from six cells). Taking into account the large standard deviations and the differences of the mean values that are found for cell preparations for different days and from different donors, the two values are not statistically different.

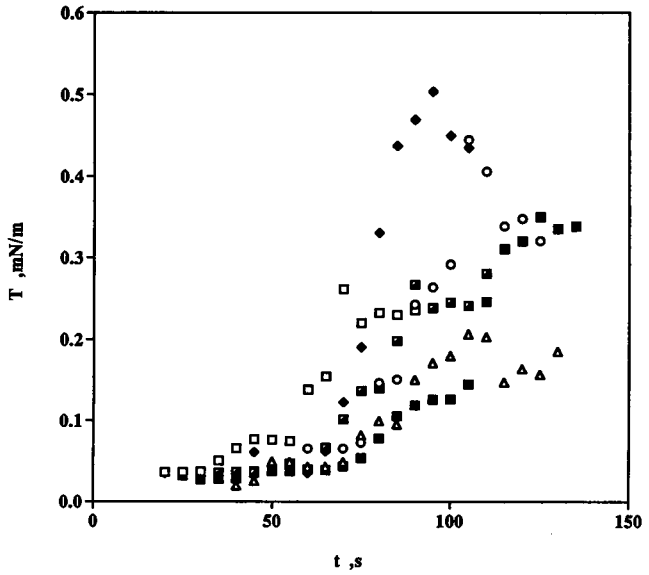

FIGURE 11 Apparent cortical tension for different cells in Ca^{2+} free media (containing EDTA) and in a medium with physiological concentration of Ca^{2+}. Different symbols are for individual cells. There is no difference in the measured apparent cortical tensions for cells in a solution containing Ca^{2+} (*triangles*, *squares*, and *diamonds*) or in a Ca^{2+} free solution (*circles*).

The differences in the measured maximum tensions and the rates of increase of the apparent cortical tension for different cells may depend on the initial state of their cytoskeleton. The following experiment was done to study this possibility. A local portion of a neutrophil was subjected to high mechanical stress and the increase of its apparent tension was measured as shown in Fig. 10. The cell was allowed to resume its spherical shape, and 5–7 min later it was subjected again to a high stress, and the change of its cortical tension measured. During the second manipulation the cortical tension was measured either in the region that was not previously subjected to a high stress (which was the region for measuring the apparent cortical tension during the first manipulation), or in the region that was previously subjected to a high stress. A total of 10 cells were measured in this experiment, with five cells for each type of measurement. The apparent cortical tensions for three cells for each type of measurement are shown in Fig. 12. When the apparent cortical tension after the second manipulation is measured in the region that was not subjected to a high stress it showed only a minor increase. When it was measured in the prestressed region, its maximum values as well as its rate of increase were similar to the ones measured during the first manipulation. This result suggests that the apparent cortical tension depends on the state of the cytoskeleton. Furthermore, it demonstrates that changes of the cytoskeleton occur in a local region and that the complete recovery of the cell requires a longer time than the waiting time (from 5 to 7 min) between two consecutive manipulations. While the contraction of the main cell body depends on the region where it is measured, there were no noticeable differences in the amount of polymerization and mass flow after the first and second manupulations in the two experiments.

DISCUSSION

Initially the shape of the neutrophil is spherical and the refractive index observed microscopically is similar for the entire surface. The surface of the resting cell is determined by the cortex (Stossel, 1982; Zhelev et al., 1994), which is under an isotropic contraction on the order of 0.024–0.035 $mN \cdot m^{-1}$ (Evans and Yeung, 1989; Needham and Hochmuth, 1992). The thickness of the cortex is on the order of 0.05–0.1 μm (Esaguy et al., 1989; Sheterline and Rickard, 1989; Zhelev et al., 1994), which is relatively small compared with the pipet radius (usually 0.3–0.4 μm). The stresses required to induce a necking instability and pull a tether depend on the yield shear resultant of the cortex (Evans and Hochmuth, 1976; Waugh, 1982). The estimate of the yield shear resultant is found from the measured maximum suction pressure for tether formation (Table 1). It is seen that at a suction pressure of 600 Pa most of the cells form cylinders inside the pipet, while at pressures above 900 Pa most of them form tethers. Therefore the critical pressure for forming a tether in a

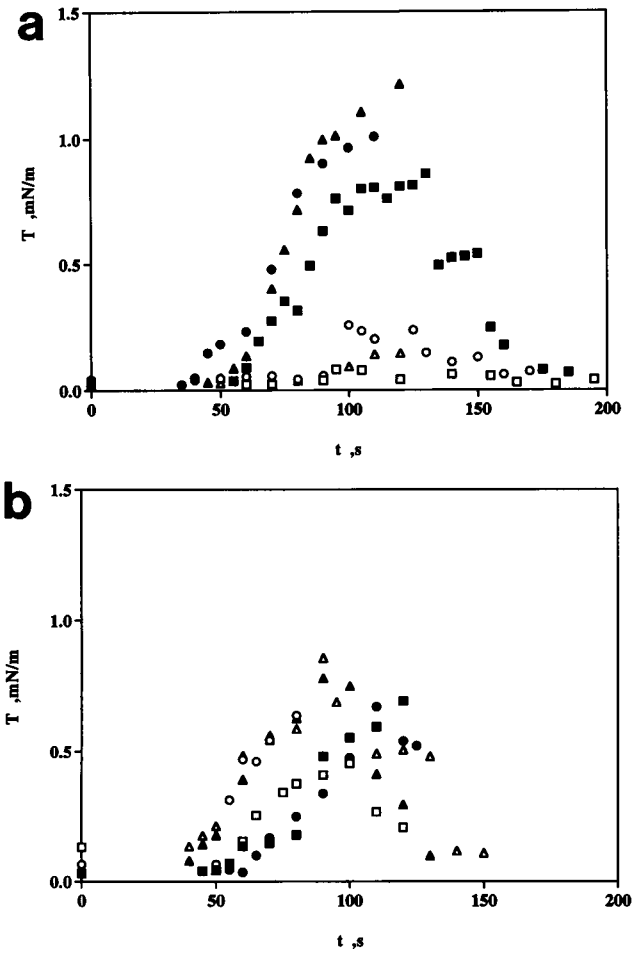

FIGURE 12 Apparent cortical tension after the first (●, ■, ▲) and the second (○, □, △) manipulations of the same cell. (*a*) During its recovery the cell is not released from the holding pipet, and the tension of its body is measured for the second time in the same region. (*b*) During its recovery the cell is held at the side of the region that has been subjected to high stress in the first manipulation. The tension of the cell body is measured in this prestressed region.

0.4-μm radius pipet is on the order of 600–900 Pa. The corresponding apparent tension is 0.12–0.18 mN·m^{-1}. The yield shear resultant is equal to half the applied tension along the axis of symmetry (Evans and Hochmuth, 1976) and thus, is 0.06–0.09 mN·m^{-1}. The upper estimate of the same quantity for the tether region (measured from the force required to keep the length of the tether constant during the first 15–20 s after its formation) is 0.04 mN·m^{-1}. The latter value is on the order of 0.02 mN·m^{-1}, which is the yield shear resultant of red cell membrane (Evans and Hochmuth, 1976; Waugh, 1982). To repeat, when the tether is released from the small pipet immediately after its formation, it retracts completely (or almost completely) back to the cell body. When it is kept in the pipet for 15–20 s or longer its length does not change (or changes in a slow process) after its release from the small pipet. The formation of a tether requires a larger shear resultant (0.06–0.09 mN·m^{-1}) compared with the one required to keep its length constant (0.04 mN·m^{-1} or less). Taken together these results suggest that during the first 15–20 s after its formation the tether is not supported by a thick cross-linked structure. Later there is a polymer structure that supports it.

The pressure difference causing neutrophil deformation into a pipet acts on the neutrophil membrane. The membrane is associated with the cortex (Pollard and Cooper, 1986; Hartwig and Kwiatkowski, 1991), which undergoes a similar deformation. The cortex is a loose structure as observed from electron micrographs of actin networks for neutrophils and macrophages (Stossel, 1982, 1993). Therefore, it is expected that during the formation of a tether most of the filaments will be oriented in the direction of the axis of symmetry. The cortex will be stretched until it yields (or breaks). When the cortex yields, its bonds break either within the filaments or at the cross-linking sites. Actin filaments, in the neutrophil cortex, are cross-linked mainly by actin-binding protein (Stossel, 1982; Gorlin et al., 1990). The amount of this protein compared with the amount of actin is 1:120 or less (Stossel, 1982). In vitro actin gels, cross-linked with actin-binding protein of the above ratio relative to the amount of actin, are very stable, and their mechanical properties resemble the ones of biotin-avidin cross-linked gels (Janmey et al., 1990). When such an actin network is deformed it shows an elastic resistance for strains up to 30%. For larger strains the network experiences irreversible deformation. Janmey et al. (1990) have concluded that the observed irreversible deformation is a result of actin filament breakage. The force required to break a single actin filament is determined by its tensile strength. The tensile strength of a single actin filament is on the order of 100 pN (Kishino and Yanagida, 1988). Therefore, the data from Table 1, together with the above considerations, may be used to determine the number of actin filaments inside the pipet during the necking instability and tether formation. The measured pulling force during necking instability and tether formation is on the order of 0.3–0.45 nN. The number of filaments in the pipet is found by dividing the pulling force by the tensile strength of a single actin filament. Then, the estimated number of filaments in the pipet is between 3 and 5. The circumference of the pipet cross-section is 2.5 μm. Therefore, the apparent number of actin filaments per 1 μm of the cell surface is between 1 and 2. The number of filaments plus the number of filament bundles per 1 μm of the cell surface found from electron micrographs of the actin networks for neutrophils and macrophages (Stossel, 1982, 1993) is on the order of 20–40. Thus, the above estimate of the number of filaments per 1 μm of the cell surface is at least 1 order of magnitude smaller than the actual number of filaments found from electron micrographs. This calculation illustrates that in contrast to the in vitro actin networks cross-linked by actin-binding protein, the neutrophil cortex is a loose, weakly cross-linked structure as suggested by other mechanical tests (Evans, 1993; Zhelev and Hochmuth, 1994).

The formation of a tether triggers spontaneous polymerization within it and within a local region around its connection to the cell surface. The measured rate of spreading of the polymerization front along the tether is on the order

of 0.07 $\mu m \cdot s^{-1}$. Another important feature is that the rate of spreading is almost constant (Fig. 3) for distances from the cell surface as far as 10–20 μm, which is larger than the cell size. This result shows that the rate is not diffusion-limited (Evans, 1993; Evans et al., 1993). Most probably it is limited by the rates of the chemical reactions in this region. The rate of spontaneous actin polymerization depends on the steady-state rates of growth of the barbed and pointed ends of the filaments. The rates of association and dissociation at 22°C of the barbed ends are on the order of 8 $s^{-1} \cdot \mu M^{-1}$ and 2 s^{-1}, and of the pointed ends are on the order of 2 $s^{-1} \cdot \mu M^{-1}$ and 1.4 s^{-1} (Pollard and Mooseker, 1981). The concentration of the globular G-actin in the cytoplasm is on the order of 120 μM (Southwick et al., 1989). Thus, the overall rates of polymerization at the barbed and at the pointed ends are on the order of 960 and 240 monomers per second, respectively. Every subunit adds 5.5 nm to the filament length (Pollard and Cooper, 1986), which gives 6.7 $\mu m \cdot s^{-1}$ for the maximum rate of growth. This is well above the measured rate of advancement of the front of polymerization, even if the effect of branching of the filaments is taken into account. Therefore, the limiting step is a process having a lower rate than the rate of actin polymerization. It is known that inside cells G-actin does not exist as a free monomer. Usually it is found as a dimer with capping and monomer binding proteins (Pollard and Cooper, 1986). The rate of polymerization inside the tether and the rate of lamellipodia spreading in phagocytosis (Evans et al., 1993) are most probably limited by the dissociation of actin dimers into monomers or by the formation of new nucleation sites for polymerization or both (Stossel, 1989, 1990, 1993). Another feature of the polymerization process is its abrupt starting and stopping. This is consistent with the stepwise movement of polarized neutrophils when the protrusion of lamellipodium, the formation of a contact with the substratum and the forward retraction of the cell body occur periodically (Cassimeris and Zigmond, 1990). Both the polymerization at a constant rate and its abrupt starting and stopping suggest that this process operates far from equilibrium (Evans, 1993).

During polymerization inside a tether, the thickness of the polymerized region does not change significantly until the polymerization front reaches the end of the tether (Fig. 2). After the whole tether is filled with a highly cross-linked material, its diameter starts to increase. Tens to hundreds of seconds later the whole cell starts to contract. This behavior is different from the one observed in phagocytosis (Evans et al., 1993), where contraction usually starts immediately after the end of spreading. The longer delay between the end of the spreading and the beginning of contraction usually occurs in longer tethers.

When a small portion of the neutrophil is subjected to large mechanical stress, polymerization begins in the prestressed region. The strains related to the applied stresses are larger than the maximum strains allowed by the adjustment of the cortical filaments. Thus, some of the filaments may break. The disrupted regions probably serve as nucleation sites for polymerization in a similar way as 1) free barbed ends, 2) barbed ends created after release of capping proteins, and 3) barbed ends created by cutting the preexisting filaments by gelsolin (Luna, 1991; Stossel, 1993). The mass flow, which starts after the initial polymerization, is driven by the pressure difference between the main cell body and the prestressed region (Fig. 9). If the cytoplasm viscosity is on the order of 50 Pa·s (which is the cytoplasm viscosity of the resting neutrophil; Hochmuth et al., 1993; Zhelev and Hochmuth, 1994), the initial pressure difference must be on the order of thousands of Pascals. The pressure difference eventually decreases to 100–150 Pa. The measured apparent tension of the main cell body during the same time interval increases continuously and reaches a maximum value on the order of 0.3–0.5 $mN \cdot m^{-1}$, which corresponds to a pressure in the cell body of 150 to 250 Pa. This value is on the order of the final values determined from flow measurements (Fig. 9). The calculated internal pressures are subject to experimental error. The internal pressures calculated from tension measurements are more accurate than the ones found from mass flow measurements. Therefore, the latter are considered only as plausible estimates of the true values. There are two significant sources of experimental error in the mass flow experiments: error from defining the "boundary" of the nozzle and error from measuring the nozzle shape. The "boundary" of the nozzle is not well defined because its shape is given by the cortical filaments. Therefore, there is a region lining the nozzle wall that excludes granules but is permeable to the cytoplasm, which contributes to the volumetric flow. When the outside diameter of the nozzle region is taken as its upper estimate, a nozzle with a diameter of 1.5 μm (which is in the middle of the interval of measured nozzle diameters in Fig. 7) will have a corrected diameter of 1.9 μm. This new diameter corresponds to an internal pressure difference that is half the current estimate of 800 Pa. When the angle characterizing the nozzle shape changes between $\pi/2.5$ and $\pi/3.5$ radians, the estimated value of 800 Pa becomes 520 Pa and 1250 Pa, respectively. It is seen that even in the worst case the internal pressures estimated from the mass flow measurements are larger than or on the same order of magnitude as the maximum internal pressures calculated from the maximum measured tensions. Another observation that is important for the understanding of this process is that the maximum pressure in the mass flow experiment is found at the beginning of the flow, which starts 30–40 s before any increase in the tension of the main cell body can be measured. The increase in the apparent tension of the main cell body starts at the middle course of the mass flow, at about 60–80 s, when the shape of the cell is best represented by Fig. 10, *b* and *c*. Furthermore, the experiments with secondary cell manipulation show that while the polymerization and mass flow are independent of both the number of manipulations and the region on the cell surface where the high stress is applied, the contraction of the cell body depends on these two factors. All these results taken together suggest that the internal pressure difference driving the mass flow can be due to the contraction of the main cell body only during the final stages of flow.

Thus, except for the final stages, the internal pressure difference that creates the flow is generated by processes located in the prestressed region. It is suggested that the prestressed region "swells" (which may be coupled with contraction), creating in this way a suction pressure. This swelling precedes the increase in the cortical tension or contraction of the main cell body. The apparent swelling of actin-myosin networks during contraction is suggested by the observation of filament twisting during the contraction of actin filaments on myosin substrates (Nishizaka et al., 1993). The swelling may also be triggered by cytosol molecules infiltrating the prestressed region. The conclusion that the prestressed region swells is supported also by observing neutrophils stained with phallacidin at different stages of the process of cytoplasm flow (Fig. 5). The intensity of the prestressed region just before the beginning of mass flow is much brighter than that observed in the later stages. This may be explained if it is assumed that the density of the polymer network before initiation of the mass flow is larger than its density in the later stages.

The cytoskeleton of resting neutrophils occupies a thin region adjacent to the cell surface (Zhelev et al., 1994). This is the structural element that provides the cortical tension. The measured tensions in Figs. 11 and 12 can be compared with the measured contraction force during phagocytosis (Evans et al., 1993), if the structural elements that provide the contraction of the main cell body remain close to the cell surface. The maximum contraction force during phagocytosis at 23°C is on the order of 12 nN. The pipet used in the experiments of Evans et al. (1993) has a diameter of 3.5 μm. Then, the apparent cortical tension, which corresponds to the measured contraction force, is 0.55 $mN \cdot m^{-1}$. This value is in excellent agreement with the measured maximum cortical tension (Figs. 11 and 12), which is on the order of 0.5 $mN \cdot m^{-1}$. The measured rate of increase of the cortical tension is on the order of 4×10^{-3} to 1.5×10^{-2} $mN \cdot m^{-1} \cdot s^{-1}$, which is similar to the rate of 7×10^{-3} $mN \cdot m^{-1} \cdot s^{-1}$ calculated in the phagocytosis experiments. Therefore, the mechanism for cell body contraction is probably the same in both experiments.

The changes experienced by the neutrophil cortex after the application of a high stress to a small portion of the cell body are local. This is seen from the cell shapes in Figs. 2, 4, and 10, and from the density distribution of the filamentous actin (Fig. 5). The local effect of these changes on the cell surface is also suggested by the observed differences in the cortical tension after the secondary manipulation of the cell (Fig. 12). The polymerization along a tether and the mechanically stimulated contraction of the cell cortex are both similar to the lamellipodia spreading and cell body contraction that are measured during phagocytosis (Evans et al., 1993). There is, however, a striking difference between the two processes because the mechanically stimulated changes occur in the absence of any external chemicals that may trigger cell activation. Even though the exact mechanism of both the mechanically stimulated cytoskeleton rearrangement and the increase of the cortical contraction is unknown, and the relation of this process to the process of phagocytosis and/or cell crawling is to be found, it is believed that the reported results give new insights into cell activation and motility.

This work was supported by grants 5 RO1 HL23728 and GM 40162 from the National Institutes of Health.

REFERENCES

Andre, P., C. Capo, A.-M. Benoliel, M. Buferne, and P. Bongrand. 1990. Analysis of the topological changes induced on cells exposed to adhesive or mechanical stimuli. *Cell Biophys.* 16:13–34.

Cassimeris, L., and S. H. Zigmond. 1990. Chemoattractant stimulation of polymorphonuclear leukocyte locomotion. *Semin. Cell Biol.* 1:125–134.

Cunningham, C. C., J. B. Gorlin, D. J. Kwiatkowski, J. H. Hartwig, P. A. Janmey, H. R. Byers, and T. P. Stossel. 1992. Actin-binding protein requirement for cortical stability and efficient locomotion. *Science* 255: 325–327.

Esaguy, N., A. P. Aguas, and M. T. Silva. 1989. High-resolution localization of lactoferrin in human neutrophils: labeling of secondary granules and cell heterogeneity. *J. Leucocyte Biol.* 46:51–62.

Evans, E. A. 1993. New physical concepts for cell amoeboid motion. *Biophys. J.* 64:1306–1322.

Evans, E. A., and R. M. Hochmuth. 1976. Membrane viscoplastic flow. *Biophys. J.* 16:13–26.

Evans, E. A., and B. Kukan. 1984. Passive material behavior of granulocytes based on large deformation and recovery after deformation tests. *Blood.* 64:1028–1035.

Evans, E., A. Leung, and D. Zhelev. 1993. Synchrony of cell spreading and contraction force as phagocytes engulf large pathogens. *J. Cell Biol.* 122: 1295–1300.

Evans, E. A., and R. Skalak. 1980. Mechanics and Thermodynamics of Biomembranes. CRC Press Inc., Boca Raton, FL.

Evans, E. A., and A. Yeung. 1989. Apparent viscosity and cortical tension of blood granulocytes determined by micropipet aspiration. *Biophys. J.* 56:151–160.

Geiger, B. 1983. Membrane-cytoskeleton interactions. *Biochim. Biophys. Acta.* 737:305–341.

Gorlin, J., R. Yamin, S. Egan, M. Stewart, T. Stossel, D. Kwiatkowski, and J. Hartwig. 1990. Human endothelial actin-binding protein (ABP-280, non-muscle filamin): a molecular leaf spring. *J. Biol. Chem.* 111:1089–1105.

Happel, J., and H. Brenner. 1986. Low Reynolds Number Hydrodynamics. Martinus Nijhoff Publishers, Dordrecht.

Hartwig, J. H., and D. J. Kwiatkowski. 1991. Actin-binding proteins. *Curr. Opin. Cell Biol.* 3:87–97.

Hartwig, J. H., R. Neiderman, and S. E. Lind. 1985. Cortical actin structures and their relationship to mammalian cell movements. *Subcellular Biochem.* 11:1–49.

Hochmuth, R. M., H. P. Ting-Beall, B. B. Beaty, D. Needham, and R. Tran-Son-Tay. 1993. Viscosity of passive human neutrophils undergoing small deformation. *Biophys. J.* 64:1596–1601.

Horoyan, M., A.-M. Benoliel, C. Capo, and P. Bongrand. 1990. Localization of calcium and microfilament changes in mechanically stressed cells. *Cell Biophys.* 17:243–256.

Janmey, P. A., S. Hvidt, J. Lamb, and T. P. Stossel. 1990. ABP-actin gels resemble covalently cross-linked networks. *Nature.* 345:89–92.

Janson, L. W., J. Kolega, and D. L. Taylor. 1991. Modulation of contraction by gelation/solation in a reconstituted motile model. *J. Cell Biol.* 114: 1005–1015.

Kishino, A., and Yanagida, T. 1988. Force measurements by micromanipulation of a single actin filament by glass needles. *Nature.* 334:74–76.

Luna, E. J. 1991. Molecular links between the cytoskeleton and membranes. *Curr. Opin. Cell Biol.* 3:120–126.

Needham, D., and R. M. Hochmuth. 1990. Rapid flow of passive neutrophils into a 4 μm pipet and measurement of cytoplasmic viscosity. *J. Biomech. Eng.* 112:269–276.

Needham, D., and R. M. Hochmuth. 1992. A sensitive measure of surface stress in the resting neutrophil. *Biophys. J.* 61:1664–1670.

Nishizaka, T., T. Yagi, Y. Tanaka, and S. Ishiwata. 1993. Right-handed rotation of an actin filament in an in vitro motile system. *Nature*. 361: 269–271.

Oliver, T., J. Lee, and K. Jacobsen. 1994. Forces exerted by locomoting cells. *Semin. Cell Biol.* 5:139–147.

Pollard, T. D., and J. A. Cooper. 1986. Actin and actin-binding proteins. A critical evaluation of mechanisms and functions. *Annu. Rev. Biochem.* 55:987–1035.

Pollard, T. D., and M. S. Mooseker. 1981. Direct measurement of actin polymerization rate constants by electron microscopy of actin filaments nucleated by isolated microvillus cores. *J. Cell Biol.* 88:654–659.

Sheterline, P., and J. E. Rickard. 1989. The cortical actin filament network of neutrophil leucocytes during phagocytosis and chemotaxis. *In* The Neutrophil: Cellular Biochemistry and Physiology. M. B. Hallett, editor. CRC Press, Boca Raton, FL. 141–165.

Southwick, F. S., G. A. Dabiri, M. Paschetto, and S. H. Zigmond. 1989. Polymorphonuclear leucocyte adherence induces actin polymerization by a transduction pathway which differs from that used by chemoattractants. *J. Cell Biol.* 109:1561–1569.

Southwick, F. S., and T. P. Stossel. 1983. Contractile proteins in leukocyte function. *Sem. Hemat.* 20:305–321.

Stossel, T. P. 1982. The structure of cortical cytoplasm. *Phil. Trans. R. Soc. Lond. B* 299:275–289.

Stossel, T. P. 1989. From signal to pseudopod. How cells control cytoplasmic actin assembly. *J. Biol. Chem.* 264:18261–18264.

Stossel, T. P. 1990. How cells crawl. *Amer. Sci.* 78:408–423.

Stossel, T. P. 1993. On the crawling of animal cells. *Science*. 260:1086–1094.

Stossel, T. P., J. H. Hartwig, H. L. Yin, and O. Stendahl. 1980. The motor of amoeboid leucocytes. *Biochem. Soc. Symp.* 45:51–63.

Ting-Beall H. P., D. Needham, and R. M. Hochmuth. 1993. Volume and osmotic properties of human neutrophils. *Blood*. 81:2774–2780.

Tran-Son-Tay, R., D. Needham, A. Yeung, and R. M. Hochmuth. 1991. Time-dependent recovery of passive neutrophils after large deformation. *Biophys. J.* 60:856–866.

Usami, S., S.-L. Wung, B. A. Skieczynski, R. Skalak, and S. Chien. 1992. Locomotion forces generated by a polymorphonuclear leukocyte. *Biophys. J.* 63:1663–1666.

Waugh, R. E. 1982. Temperature dependence of the yield shear resultant and the plastic viscosity coefficient of erythrocyte membrane. *Biophys. J.* 39:273–278.

Waugh, R. E., and R. M. Hochmuth. 1987. Mechanical equilibrium of thick, hollow, liquid membrane cylinders. *Biophys. J.* 52:391–400.

Zafran, Y., H. Lepidi, A.-M. Benoliel, C. Capo, and P. Bongrand. 1993. Role of calcium in the shape control of human granulocytes. *Blood Cells* 19: 115–131.

Zhelev, D. V., D. Needham, and R. M. Hochmuth. 1994. Role of the membrane cortex in neutrophil deformation in small pipets. *Biophys. J.* 67: 696–705.

Zhelev, D. V., and R. M. Hochmuth. 1994. Human neutrophils under mechanical stress. *In* Cellular Mechanics and Cellular Engineering. V. C. Mow, F. Guilak, R. Tran-Son-Tay, and R. M. Hochmuth, editors. Springer-Verlag, New York. 3–21.